



Figures and figure supplements

BubR1 alterations that reinforce mitotic surveillance act against aneuploidy and cancer

Robbyn L Weaver et al

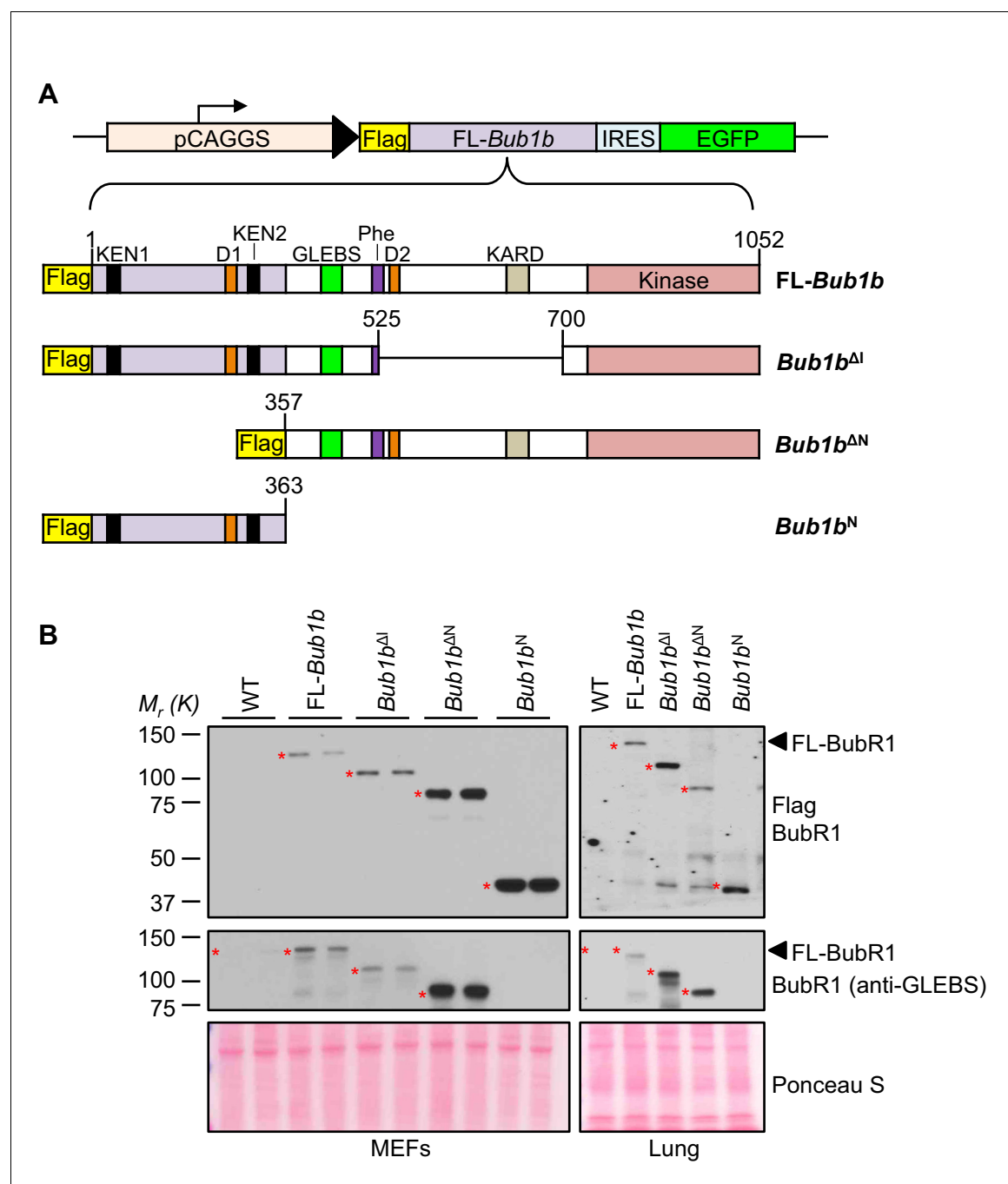


Figure 1. BubR1 transgenic mutant proteins are highly overexpressed in vitro and in vivo. (A) (top) *Bub1b* transgenic vector design. pCAGGS, promoter consisting of the CMV immediate enhancer and the chicken-actin promoter. FL, full-length. IRES, internal ribosome entry site. (bottom) Schematics of the Flag-*Bub1b* transgenic mouse constructs. KEN, KEN-box. D, destruction-(D-)box. GLEBS, GLEBS-binding motif. Phe, Phe box. KARD, kinetochore attachment regulatory domain. (B) Western blots of MEF (left) and lung tissue extracts (right) from wild-type (WT) and Flag-*Bub1b* transgenic mice. Blots were probed with the indicated antibodies. Ponceau S was used to normalize loading.

DOI: [10.7554/eLife.16620.003](https://doi.org/10.7554/eLife.16620.003)

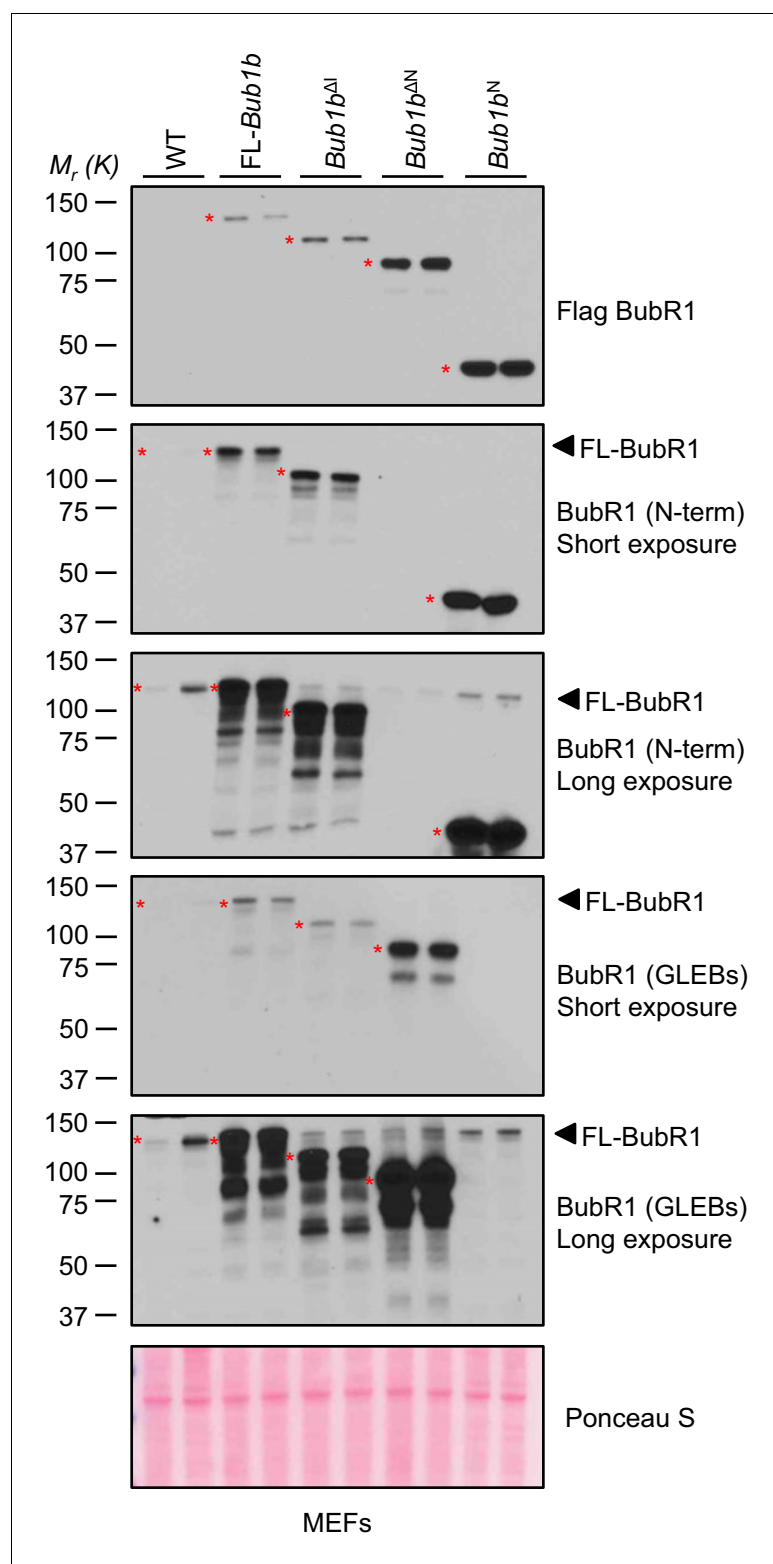


Figure 1—figure supplement 1. Analysis of BubR1 overexpression in transgenic MEFs. Full scan and multiple exposures of Western blots of MEF lysates from **Figure 1B**. WT, wild-type. FL, full-length.

DOI: [10.7554/eLife.16620.004](https://doi.org/10.7554/eLife.16620.004)

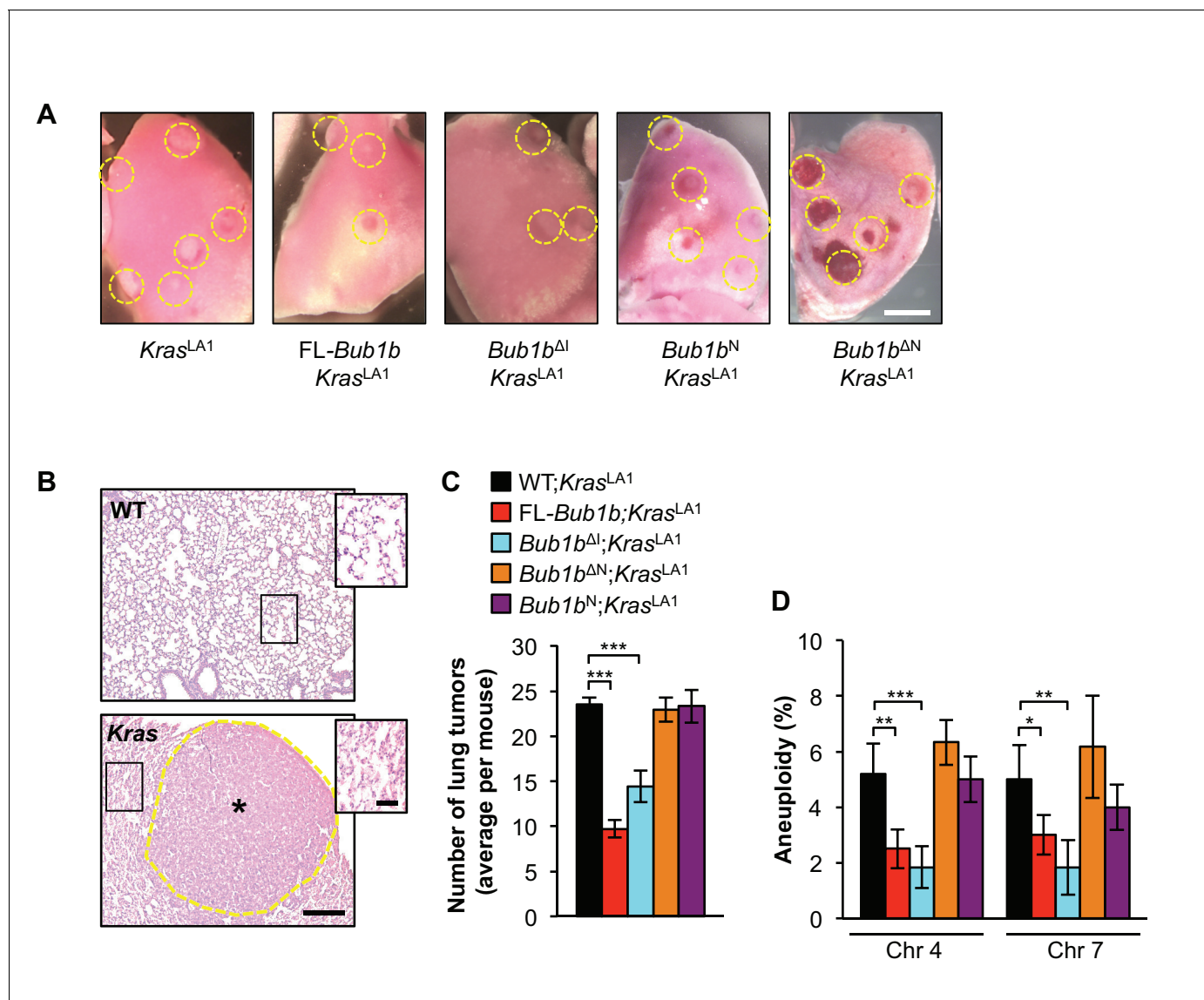


Figure 2. Select BubR1 domain overexpression protects against aneuploidy and cancer. (A) Lung lobes of *Kras^{LA1}* mice and *Kras^{LA1}* mice expressing various BubR1 transgenic proteins sacrificed at 6 weeks of age. Entire lungs were inspected using a dissection microscope to quantitate the number of lung tumors (adenomas) per mouse. (B) Hematoxylin-eosin stained lung sections of representative normal (WT) lung and a *Kras^{LA1}* (*Kras*) hyperplastic tumor-bearing lung (the dashed line marks the adenoma boundary). Insets highlight normal and hyperplastic lung architecture. (C) Quantification of the number of lung tumors from mice shown in A. $n = 20$, except for full-length (FL)-*Bub1b* where $n = 7$. Data are mean \pm s.e.m. *** $p < 0.001$. (D) Interphase FISH on the lungs of wild-type and *Kras^{LA1}* with and without FL-*Bub1b* and mutant overexpression. $n = 5$, ≥ 100 cells per animal. Data are mean \pm s.d. * $p < 0.05$, ** $p < 0.01$, *** $p < 0.001$. Scale bars: A, 2 mm; B, 200 μ m (main image) and 50 μ m (insets). (See associated **Figure 2—source data 1**). DOI: 10.7554/eLife.16620.011

The following source data is available for figure 2:

Source data 1. Source file for tumor incidence and tissue aneuploidy rate data.

DOI: 10.7554/eLife.16620.012

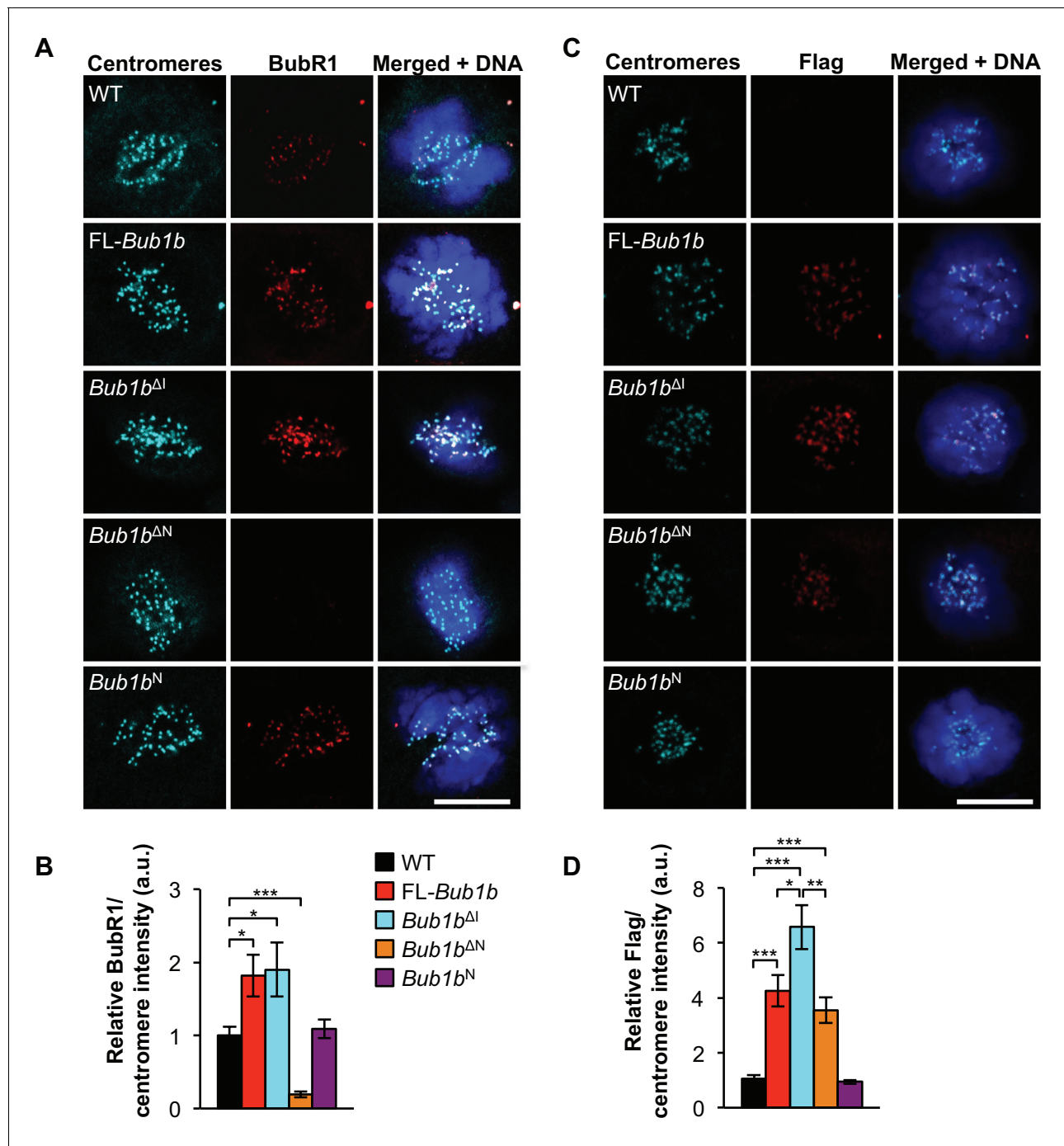


Figure 3. Increased BubR1 localization to kinetochore corresponds to phenotypic benefits. (A) MEFs of indicated genotypes were stained for BubR1 (red), centromeres (cyan), and DNA (blue). WT, wild-type. FL, full-length. (B) Quantification of immunostaining of BubR1 shown in A. Values were normalized to centromere stain and are relative to wild-type. $n = 3$ lines, ≥ 10 cells per line. Data are mean \pm s.d. * $p < 0.05$, *** $p < 0.001$. (C) Same as in A except with anti-Flag antibody to detect transgenic BubR1. (D) Quantification of immunostaining of Flag shown in C. Values were normalized to centromere stain and are relative to wild-type. Wild-type and *Bub1b*^N represent background. $n = 3$ lines, ≥ 10 cells per line. Data are mean \pm s.d. * $p < 0.05$, ** $p < 0.01$, *** $p < 0.001$. Scale bar 10 μ m. (See associated **Figure 3—source data 1**).

DOI: [10.7554/eLife.16620.013](https://doi.org/10.7554/eLife.16620.013)

The following source data is available for figure 3:

Source data 1. Source file for intensity of kinetochore-localized BubR1 and FLAG protein data.

DOI: [10.7554/eLife.16620.014](https://doi.org/10.7554/eLife.16620.014)

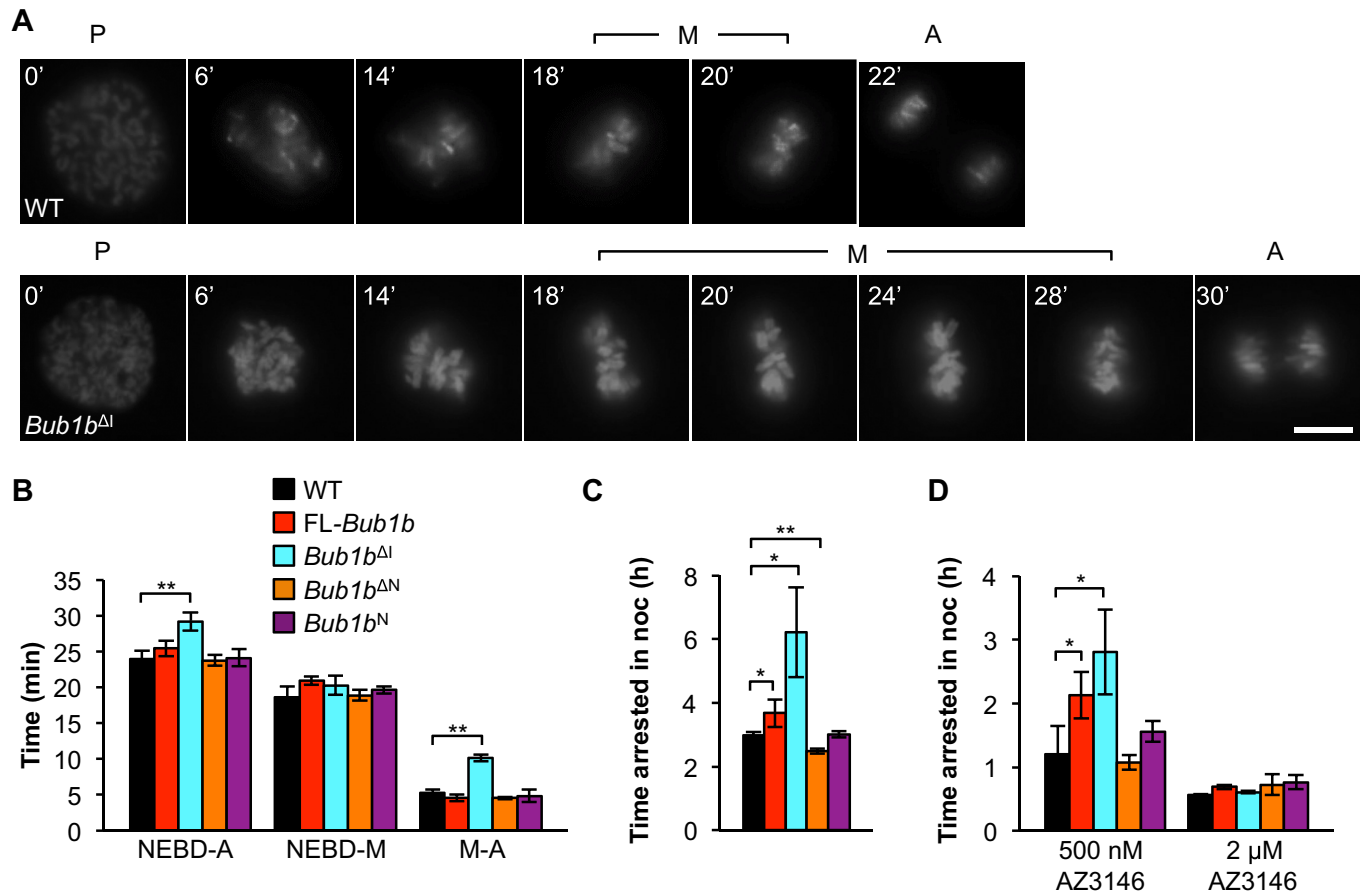


Figure 4. *Bub1b^{ΔI}* MEFs have an increased time in mitosis and duration of mitotic arrest. (A) Representative time-lapse images of live MEF cells of indicated genotypes progressing from prophase (t = 0) to anaphase (A). Time is indicated in min. WT, wild-type. P, prophase. M, metaphase. (B) Analysis of the time from nuclear envelope breakdown (NEBD) to anaphase onset in H2B-RFP MEFs of the indicated genotypes by live cell time-lapse imaging. $n = 3$ lines, ≥ 20 cells per line. Data are mean \pm s.d. $**p < 0.01$. FL, full-length. (C) In a nocodazole challenge, H2B-RFP MEFs of indicated genotypes were treated with 100 ng/ml of nocodazole (noc) and monitored by live cell time-lapse imaging. The point of time in which 50% of cells are arrested in mitosis is plotted. $n \geq 3$ lines, ≥ 20 cells per line. Data are mean \pm s.d. $*p < 0.05$, $**p < 0.01$. (D) H2B-RFP wild-type and mutant transgenic MEFs were treated concurrently with 100 ng/ml nocodazole and indicated concentrations of the Mps1 kinase inhibitor, AZ3146. The point of time in which 50% of cells are arrested in mitosis is plotted. $n = 3$ lines, ≥ 20 cells per line. Data are mean \pm s.d. $*p < 0.05$. Scale bar, 10 μ m (See associated [Figure 4—source data 1](#)).

DOI: [10.7554/eLife.16620.015](https://doi.org/10.7554/eLife.16620.015)

The following source data is available for figure 4:

Source data 1. Source file for mitotic timing and nocodazole arrest data.

DOI: [10.7554/eLife.16620.016](https://doi.org/10.7554/eLife.16620.016)



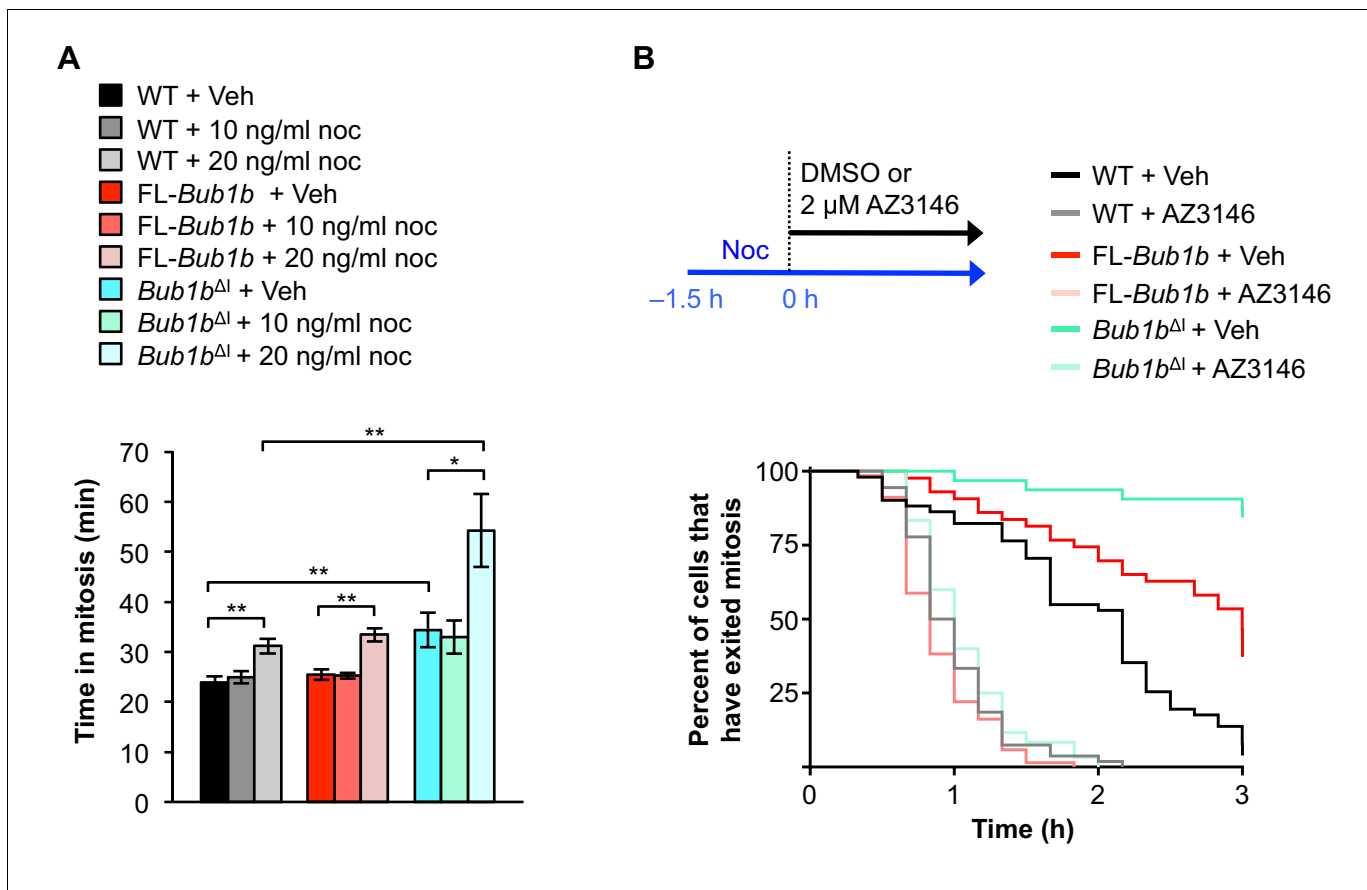


Figure 5. *Bub1b*^{Δl} MEFs have a lower threshold to checkpoint activation. (A) Analysis of the time from NEBD to anaphase onset in H2B-RFP MEFs of the indicated genotypes treated with either DMSO vehicle (Veh) or indicated concentration of nocodazole (Noc). $n = 3$ lines, ≥ 20 cells per line. Data are mean \pm s.d. * $p < 0.05$, ** $p < 0.01$. WT, wild-type. FL, full-length. (B) (top) Strategy for analyzing the checkpoint silencing efficiency. MEFs of indicated genotypes were treated with 100 ng/ml nocodazole for 1.5 hr before addition of either DMSO vehicle (Veh) or 2 μ M AZ3146, at which point cells were marked and monitored for time of escape (time point zero). (bottom) Analysis of duration of mitotic arrest from time point zero as outlined in (top). $n = 3$ lines, ≥ 20 cells per line. (See associated **Figure 5—source data 1**).

DOI: [10.7554/eLife.16620.018](https://doi.org/10.7554/eLife.16620.018)

The following source data is available for figure 5:

Source data 1. Source file for low-dose nocodazole challenge and SAC silencing data.

DOI: [10.7554/eLife.16620.019](https://doi.org/10.7554/eLife.16620.019)

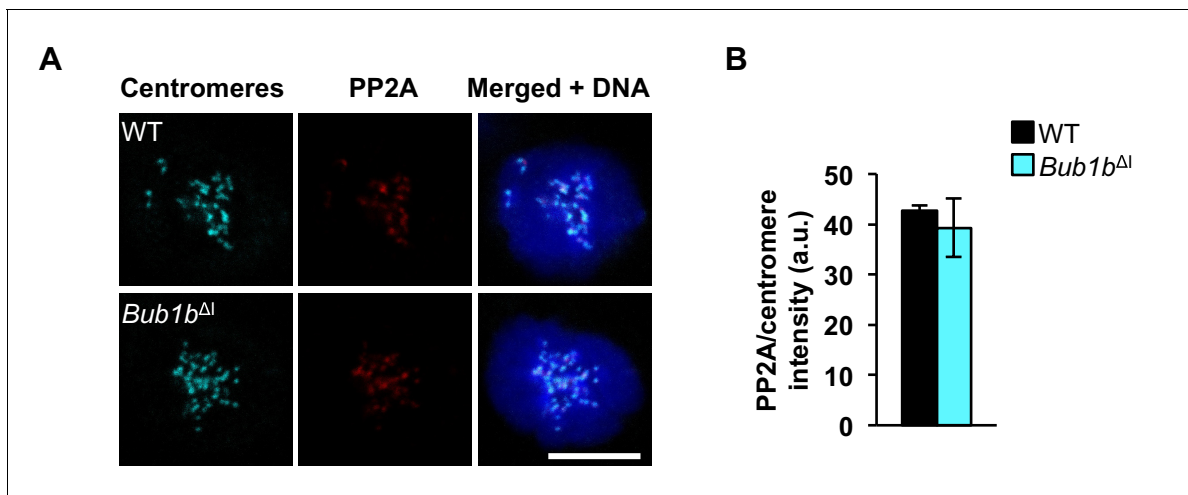


Figure 5—figure supplement 1. PP2A localization is normal in *Bub1b*^{Δl} MEFs. (A) Wild-type (WT) and *Bub1b*^{Δl} MEFs were arrested in 100 ng/ml nocodazole and stained for PP2A (red), centromeres (cyan), and DNA (blue). (B) Quantification of immunostaining of PP2A in A. Values were normalized to centromere stain. $n = 3$ lines, ≥ 10 cells per line. Data are mean \pm s.d. Scale bar 10 μ m. (See associated **Figure 5—figure supplement 1—source data 1**).

DOI: [10.7554/eLife.16620.020](https://doi.org/10.7554/eLife.16620.020)

The following source data is available for figure 5:

Figure supplement 1—Source data 1. Source file for intensity of kinetochore-localized PP2A protein data.

DOI: [10.7554/eLife.16620.021](https://doi.org/10.7554/eLife.16620.021)

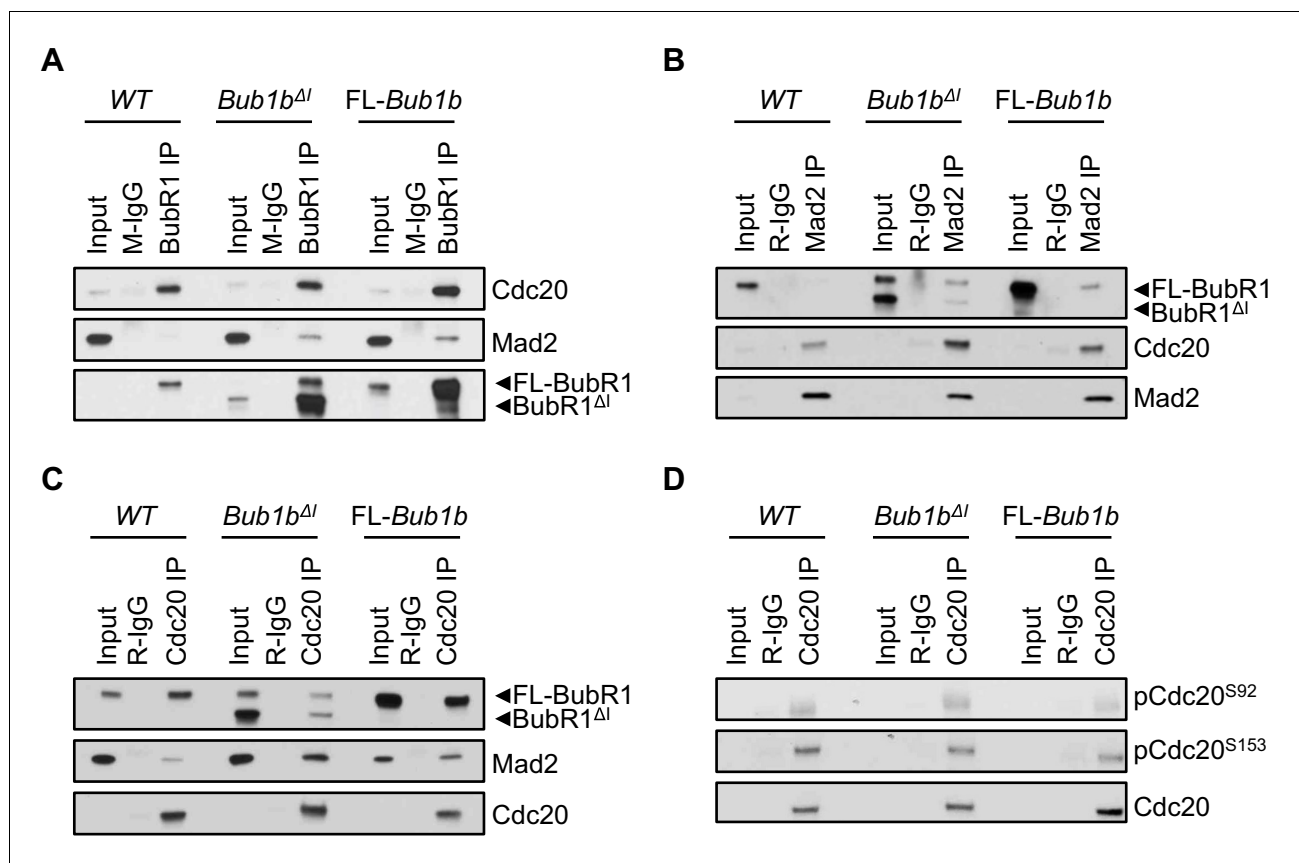


Figure 6. Composition of mitotic checkpoint complexes is unique in *Bub1b* ΔI MEFs. (A–D) Immunoblots of mitotic wild-type (WT) and indicated mutant MEF extracts subjected to co-immunoprecipitation with the indicated antibodies. Each blot is a representative of at least 3 experiments. FL, full-length. DOI: [10.7554/eLife.16620.022](https://doi.org/10.7554/eLife.16620.022)

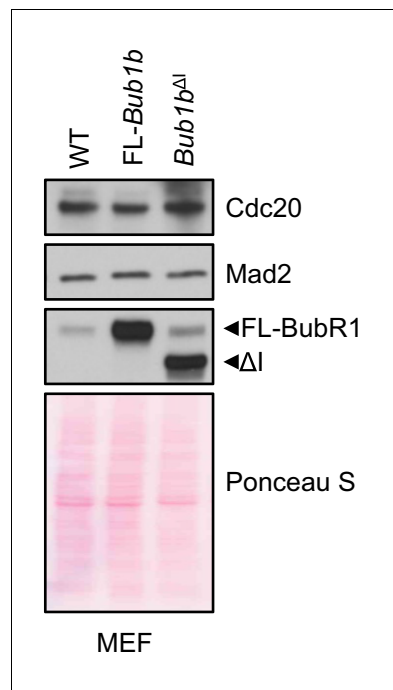


Figure 6—figure supplement 1. Mitotic checkpoint components have a normal expression in *Bub1b* transgenic MEFs. Western blot analysis of mitotic MEF lysates of indicated genotypes. Blots were probed with indicated antibodies. Ponceau S was used to normalize loading. Blot is a representative of at least three experiments. WT, wild-type. FL, full-length.
[DOI: 10.7554/eLife.16620.023](https://doi.org/10.7554/eLife.16620.023)

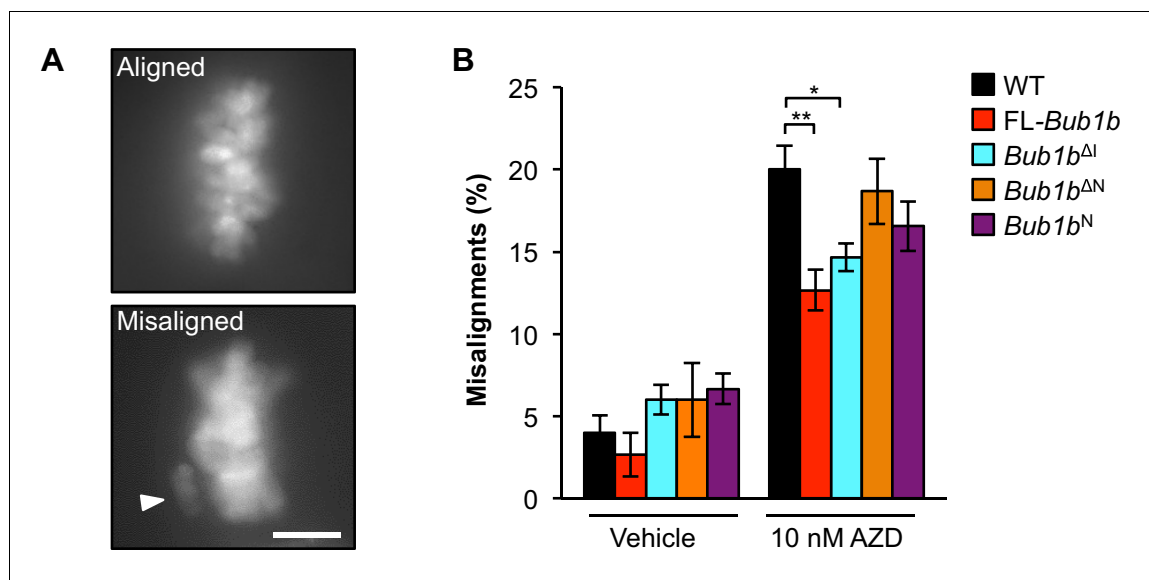


Figure 7. Overexpression of FL-BubR1 and BubR1^{ΔI} improves error correction rates. **(A)** Representative images of MEFs with aligned or misaligned chromosomes after monastrol washout. White arrowhead depicts misaligned chromosome. **(B)** Analysis of chromosome misalignment in MEFs expressing the indicated *Bub1b* transgenes. MEFs were treated with 100 μ M monastrol for 1 hr and then with monastrol and 10 μ M MG132 for 1 hr and released for 90 min into MG132. Cells were treated with DMSO (Vehicle) or 10 nM AZD1152-HQPA (AZD) throughout the duration of the experiment. $n = 6$ lines (≥ 25 cells per line were analyzed). Data are mean \pm s.d. * $p < 0.05$, ** $p < 0.01$. Scale bar, 10 μ m. WT, wild-type. (See associated **Figure 7—source data 1**).

DOI: [10.7554/eLife.16620.024](https://doi.org/10.7554/eLife.16620.024)

The following source data is available for figure 7:

Source data 1. Source file for monastrol washout data.

DOI: [10.7554/eLife.16620.025](https://doi.org/10.7554/eLife.16620.025)

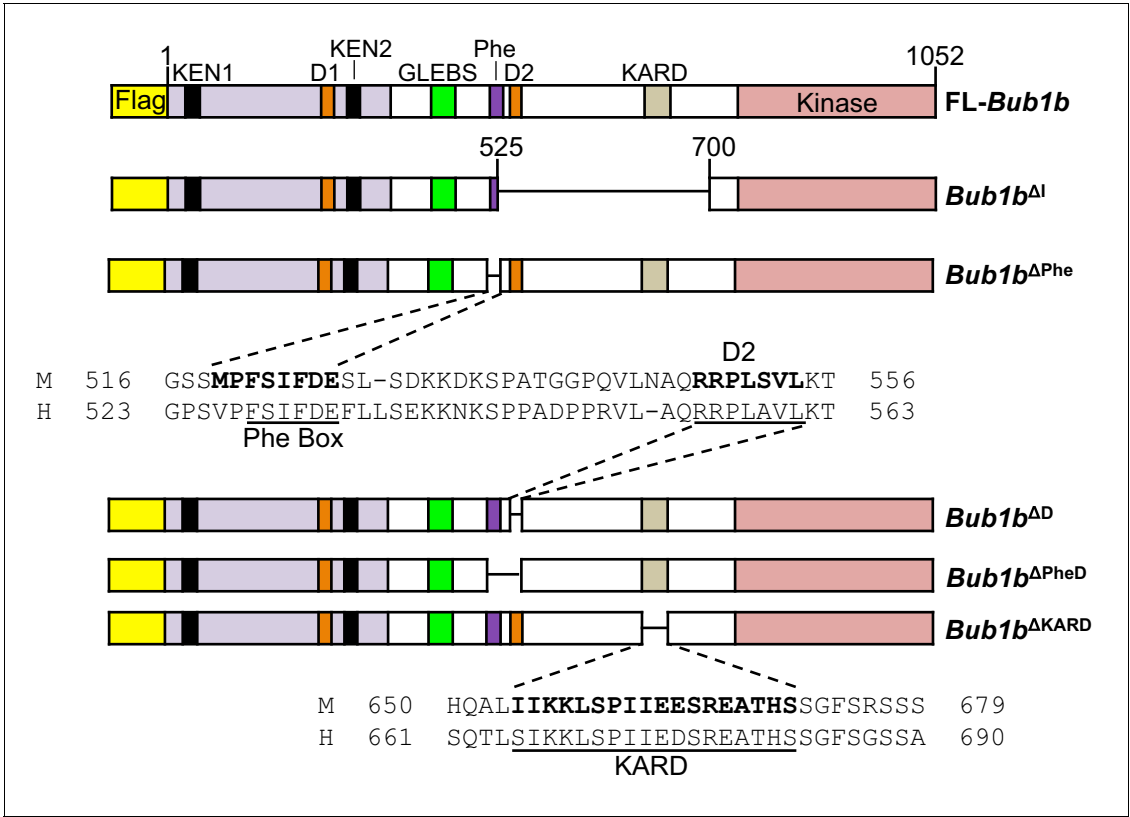


Figure 8. Schematics of pTripZ-Flag-Bub1b mutants. Schematics of the pTripZ-Flag-Bub1b constructs. D, destruction-(D-)box. GLEBs, GLEBs-binding motif. Phe, Phe box. KARD, kinetochore attachment regulatory domain. FL, full-length. Sequence alignment of the Phe box, D-box2, and KARD region of human and mouse BubR1. Residues characterized in human BubR1 are underlined, and homologous residues deleted in mouse Bub1b constructs are bold.

DOI: 10.7554/eLife.16620.026

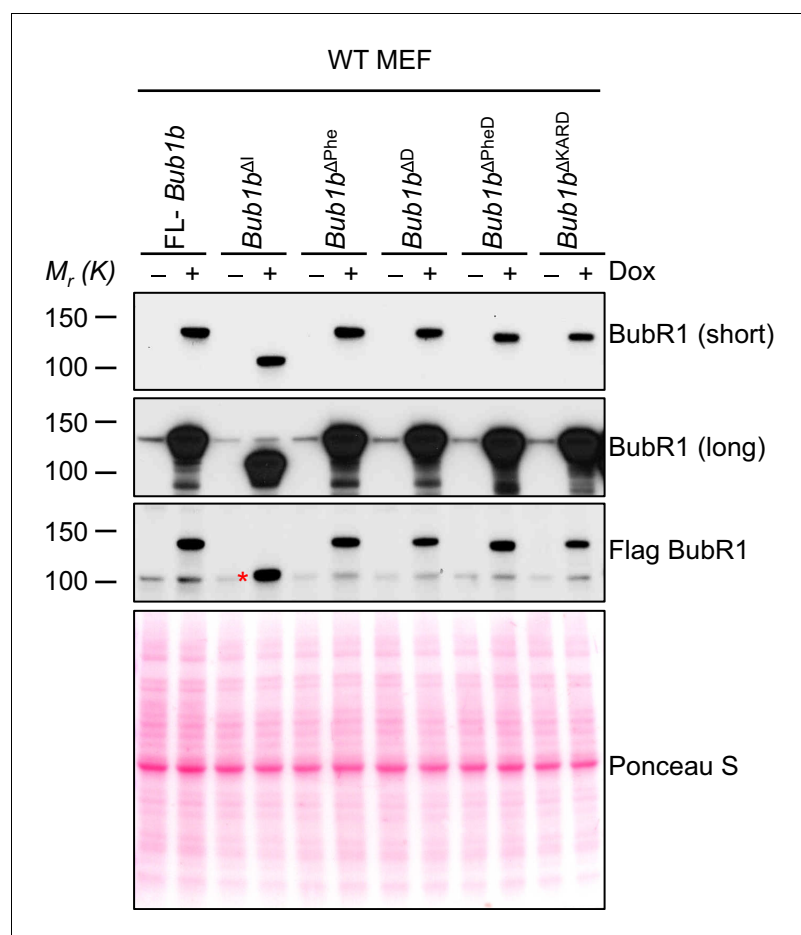


Figure 8—figure supplement 1. Protein levels of *Bub1b* deletion constructs in wild-type MEFs. Western blots of wild-type (WT) MEFs infected with the indicated constructs with or without doxycycline (Dox). Blots were probed with the indicated antibodies. Ponceau S was used to normalize loading. Asterisk indicates specific band for *BubR1*^{ΔI}.

DOI: [10.7554/eLife.16620.027](https://doi.org/10.7554/eLife.16620.027)

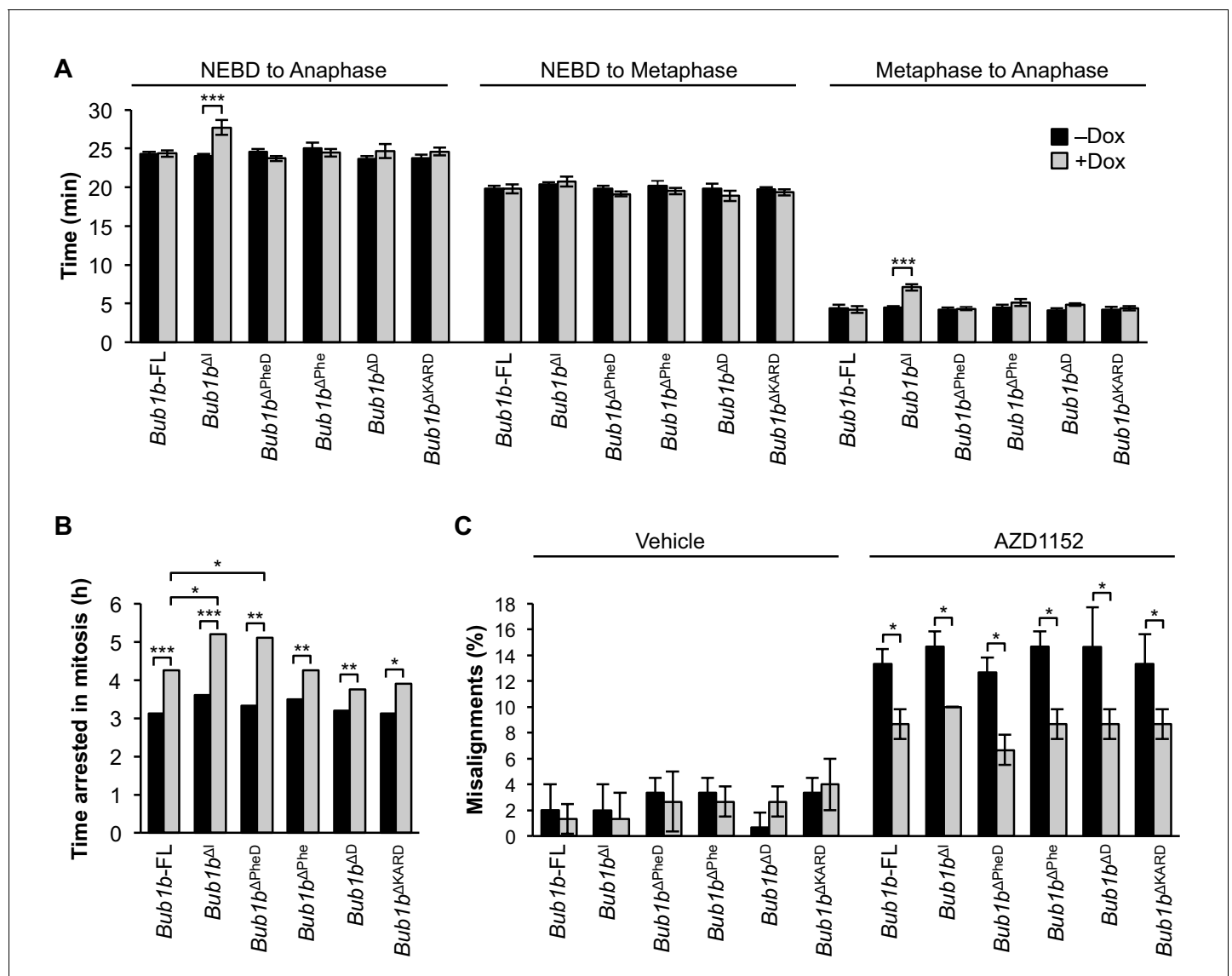


Figure 9. BubR1 deletion constructs extend nocodazole arrest and positively impact error attachment machinery. (A) Analysis of the time from nuclear envelope breakdown (NEBD) to anaphase onset in H2B-RFP wild-type MEFs infected with the indicated constructs with and without the addition of doxycycline (Dox) by live cell time-lapse imaging. $n = 1$ line, ≥ 20 cells per treatment. Data are mean \pm s.e.m. *** $p < 0.001$. FL, full-length. (B) In a nocodazole challenge, H2B-RFP wild-type MEFs infected with the indicated constructs with and without the addition of Dox were treated with 100 ng/ml of nocodazole and monitored by live cell time-lapse imaging. The point of time in which 50% of cells are arrested in mitosis is plotted. $n = 1$ line, ≥ 15 cells per treatment. * $p < 0.05$, ** $p < 0.01$, *** $p < 0.001$. (C) Analysis of chromosome misalignment in wild-type MEFs infected with the indicated constructs with and without addition of Dox. MEFs were treated with 100 μ M monastrol for 1 hr and then with monastrol and 10 μ M MG132 for 1 hr and released for 90 min into MG132. Cells were treated with DMSO (Vehicle) or 50 nM AZD1152-HQPA (AZD1152) throughout the duration of the experiment. $n = 3$ lines, 50 cells per line per treatment. Data are mean \pm s.d. * $p < 0.05$. (See associated [Figure 9—source data 1](#)).

DOI: [10.7554/eLife.16620.028](https://doi.org/10.7554/eLife.16620.028)

The following source data is available for figure 9:

Source data 1. Source file for mitotic timing, nocodazole challenge and monastrol washout data.

DOI: [10.7554/eLife.16620.029](https://doi.org/10.7554/eLife.16620.029)

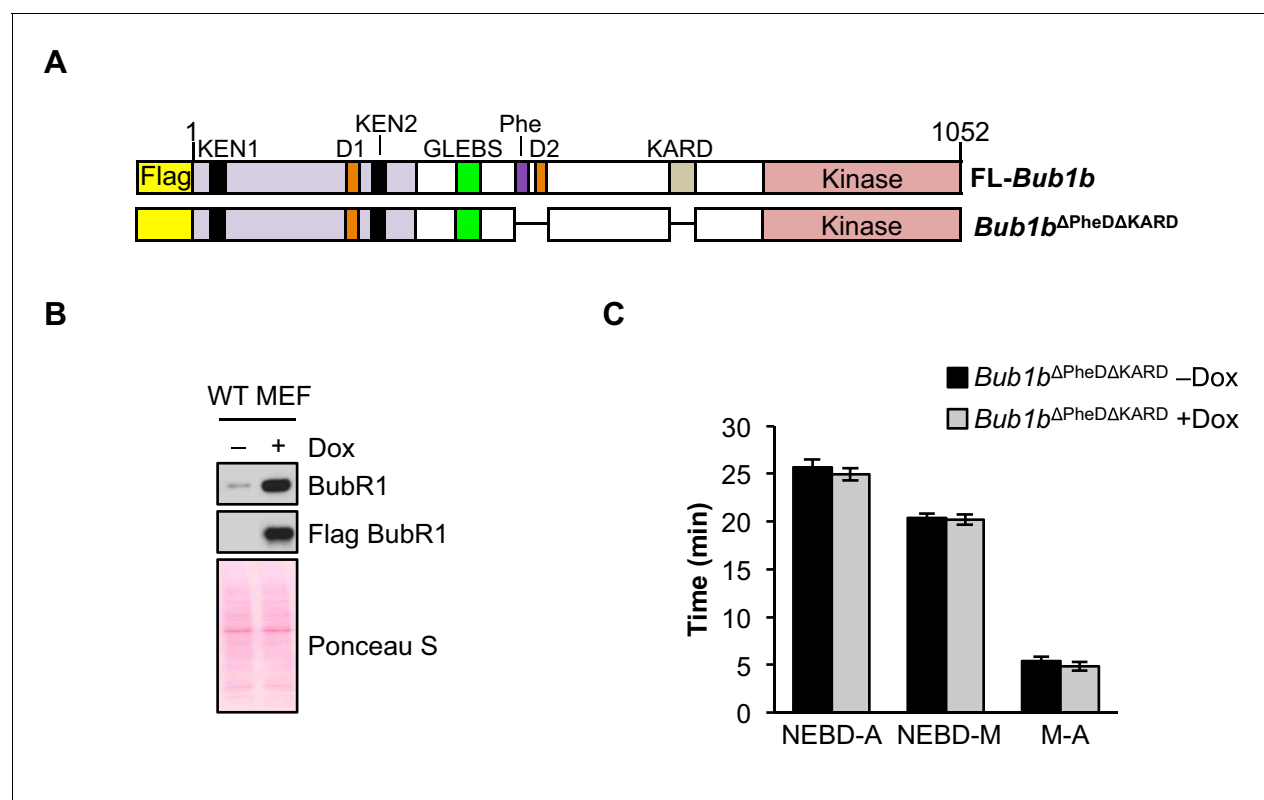


Figure 9—figure supplement 1. Combined loss of Phe, D-box2 and KARD does not impact mitotic timing. (A) Schematic of the pTripZ-Flag-*Bub1b*^{ΔPheDAKARD} construct. D, destruction-(D-)box. GLEBs, GLEBs-binding motif. Phe, Phe box. KARD, kinetochore attachment regulatory domain. FL, full length. (B) Western blot of wild-type (WT) MEFs infected with *Bub1b*^{ΔPheDAKARD} with or without doxycycline (Dox). Blot was probed with the indicated antibodies. Ponceau S was used to normalize loading. (C) Analysis of the time from nuclear envelope breakdown (NEBD) to anaphase onset in H2B-RFP WT MEFs infected with *Bub1b*^{ΔPheDAKARD} with and without the addition of Dox by live cell time-lapse imaging. $n = 1$ line, ≥ 20 cells. Data are mean \pm s.e.m. M, metaphase. (See associated **Figure 9—figure supplement 1—source data 1**).

DOI: [10.7554/eLife.16620.030](https://doi.org/10.7554/eLife.16620.030)

The following source data is available for figure 9:

Figure supplement 1—Source data 1. Source file for mitotic timing data.

DOI: [10.7554/eLife.16620.031](https://doi.org/10.7554/eLife.16620.031)

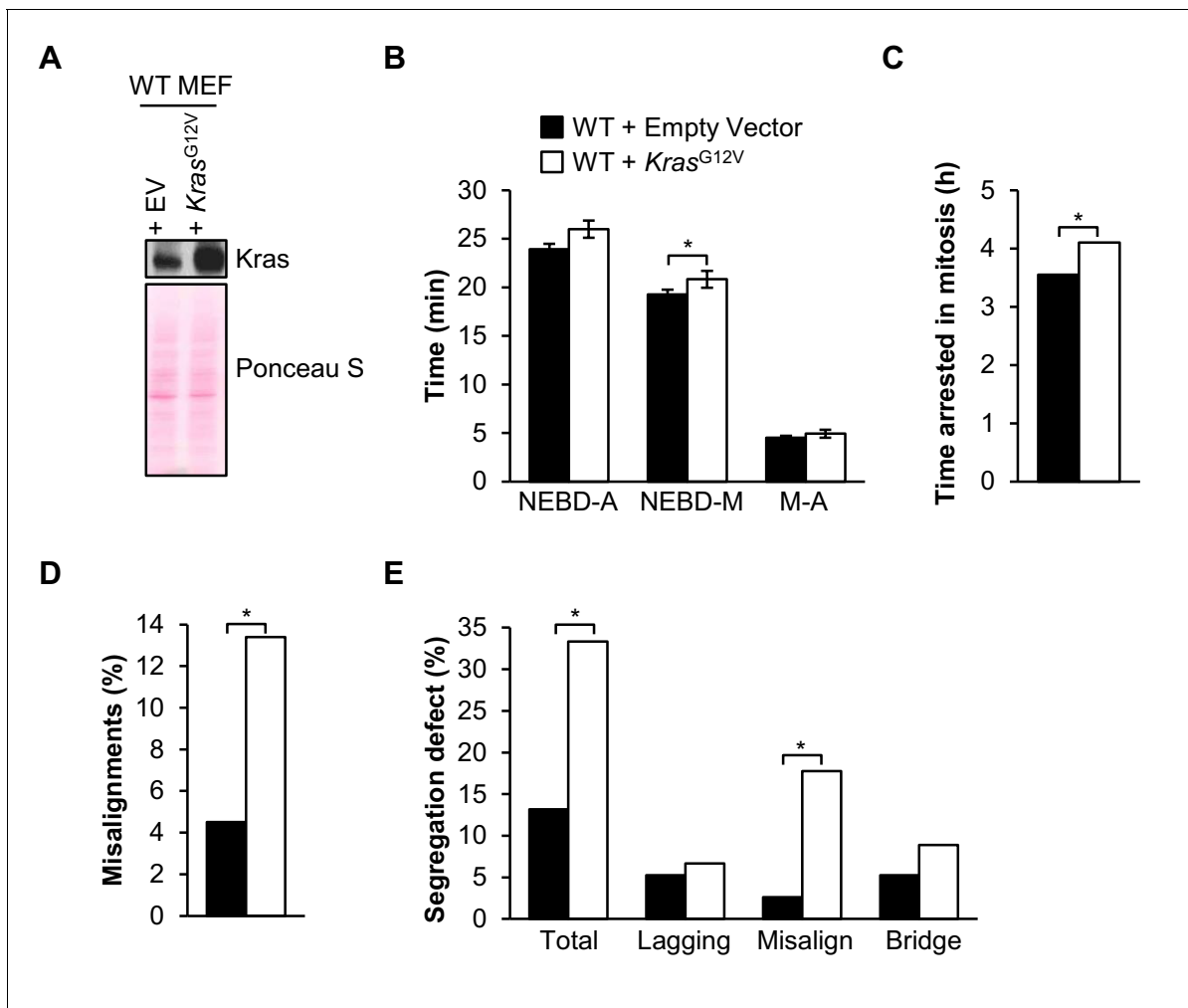


Figure 10. Oncogenic Kras increases microtubule-kinetochore malattachment. (A) Western blot of wild-type (WT) MEFs infected with pBABE-Puro-KRas (G12V) or empty vector (EV). Blot was probed with the indicated antibody. Ponceau S was used to normalize loading. (B) Analysis of the time from nuclear envelope breakdown (NEBD) to anaphase (A) onset in H2B-RFP wild-type MEFs infected with *Kras*^{G12V} or EV by live cell time-lapse imaging. *n* = 1 line, ≥ 19 cells. Data are mean ± s.d. **p* < 0.05. M, metaphase (C) In a nocodazole challenge, H2B-RFP wild-type MEFs infected with *Kras*^{G12V} or EV were treated with 100 ng/ml of nocodazole and monitored by live cell time-lapse imaging. The point of time in which 50% of cells are arrested in mitosis is plotted. *n* = 1 line, ≥ 20 cells. **p* < 0.05. (D) Analysis of chromosome misalignments in wild-type MEFs infected with *Kras*^{G12V} or EV. MEFs were treated with 100 μM monastrol for 1 hr and then with monastrol and 10 μM MG132 for 1 hr and released for 90 min into MG132. *n* = 1 line, ≈ 200 cells. **p* < 0.05. (E) Live-cell imaging of chromosome segregation defects in primary H2B-RFP wild-type MEFs infected with *Kras* or EV. *n* = 1 line, ≈ 40 cells. **p* < 0.05. (See associated **Figure 10—source data 1**).

DOI: [10.7554/eLife.16620.032](https://doi.org/10.7554/eLife.16620.032)

The following source data is available for figure 10:

Source data 1. Source file for mitotic timing, nocodazole challenge, missegregation assay and monastrol washout data.

DOI: [10.7554/eLife.16620.033](https://doi.org/10.7554/eLife.16620.033)